

Fetal dosimetry for ^{18}F -FDG PET Imaging during pregnancy: a comparative Monte Carlo study

Nadia Zarghi¹, Hashem Miri-Hakimabad^{1*}, Elie Hoseinian-Azghadi¹, Najmeh Mohammadi²

1. Physics Department, Faculty of Science, Ferdowsi University of Mashhad, Mashhad, Iran.

2. Physics Department, Faculty of Science, Sahand University of Technology, Tabriz, Iran

ARTICLE INFO	ABSTRACT
Article type: Original Paper	Introduction: Current reported values of fetal doses from ^{18}F Fluorodeoxyglucose (FDG) in pregnant women imaged with PET scan showed a significant variation. This study aimed to evaluate fetal radiation doses using the last generation of computational pregnant phantoms and also to shed light on one of the uncertainty components of the fetal dose.
Article history: Received: Sep 24, 2020 Accepted: Dec 26, 2020	Material and Methods: In this respect, we used a boundary representation (BREP) series of computational pregnant phantoms to evaluate radiation doses to the fetus. We also reviewed available data on fetal time-integrated activities and evaluated the confidence and prediction (95%) intervals for the existing data. By doing this, the uncertainty of fetal Biokinetic data was taken into account in fetal dose calculations.
Keywords: ^{18}F -FDG PET Imaging Radiation Dosimetry Pregnancy	Results: The fetal doses of 2.30E-02, 1.53E-02, and 1.02E-02 mGy/MBq at 3, 6 and 9 months of gestation were estimated. The results also showed the contributions of source organs to the fetal doses. The maternal "urinary bladder contents" and "other organs and tissues" are the main source regions contributing to fetal dose. We also indicated that the Biokinetic variation caused a large uncertainty on fetal dose (with a prediction interval from 1.73E-02 to 3.93E-02 mGy/MBq) at the first trimester of pregnancy, while it is much lower at second and third trimesters. Furthermore, it is indicated that variations on fetal dose outside the determined intervals may be related to the geometrical differences of used computational phantoms.
	Conclusion: Since the fetal dose is much higher and the radiation exposure is more deterministic at the first trimester of pregnancy, attempting to evaluate the fetal dose is relevant at this stage accurately.

► Please cite this article as:

Zarghi N, Miri-Hakimabad H, Hoseinian-Azghadi E, Mohammadi N. Fetal dosimetry for ^{18}F -FDG PET Imaging during pregnancy: a comparative Monte Carlo study. Iran J Med Phys 2021; 18: 461-467. 10.22038/IJMP.2020.52305.1860.

Introduction

^{18}F -FDG is the most commonly used radiotracer in positron emission tomography (PET) imaging [1]. In the last two decades, PET scans played a critical role in the clinical management of many types of cancer [2-4]. According to the RAZAVI hospital officials, a total of 8000 patients had undergone PET scans from 2015 to 2020, only in this hospital in Mashhad, Iran. However, there are no official statistics on the number of scanned pregnant patients per year. There are increased reports of pregnant patients imaged with PET; however, it still remains a rare clinical condition [5, 6].

Considering that prenatal exposure to ionizing radiation has deterministic effects on the fetus, there are concerns about the radiation dose received by pregnant patients and their unborn children. Therefore, pregnant patients are included in radiosensitive subgroups of a population and performing computational dosimetry are helpful to predict the radiation dose before any kind of medical diagnostic exposure.

To date, several studies estimated a relatively wide range of fetal radiation doses from ^{18}F -FDG PET scans. The range of fetal doses covers from about 0.3E-3 to

4.0E-2 mGy/MBq [7]. All of the previous studies stated that the fetal absorbed doses from ^{18}F -FDG PET scan remained well within safe levels and pregnancy is no contraindication to PET imaging. The key point here is that the variability of reported fetal doses raises two important questions. Firstly, one might ask where these uncertainties on fetal doses originate from; different fetal uptakes of the radiopharmaceutical, different fetal body habitus, or variation on mean distances between fetal body and maternal main source organs such as urinary bladder content. Furthermore, are all these factors equally important or one of them playing the role. Thus, which factor should be considered when one performs individual fetal dosimetry for a pregnant patient?

Secondly, by considering the variability on fetal dose estimates, is it relevant to perform dosimetric calculations more precisely? Answering these questions is not straightforward, however this study is a starting point for rigorous uncertainty analysis of the problem. This challenge needs an understanding of radiation deterministic and stochastic effects on the unborn child. Therefore, one could determine whether

assessing the fetal radiation dose at the organ level is essential or not.

The purpose of this study is to determine the fetal doses using last generation of pregnant phantoms and evaluate the effect of Biokinetic variation of ^{18}F -FDG (based on human data) on fetal radiation doses. Also we aimed to explore the above mentioned questions and find a more straightforward answer to them. Finally, whatever the magnitude of the estimated dose, it would be helpful to accurately know the amount of fetal radiation dose and its possible variations for a nuclear medicine practitioner to predict the deterministic/stochastic effects of radiation on the unborn child.

Materials and Methods

Pregnant reference phantoms

The recently developed pregnant reference phantoms were used in this study [8-10]. The phantoms are the updated version of pregnant models. Each fetal model contains 21 different organs and tissues including the age-dependent details of fetal cartilaginous and ossified bones. The original version of the phantoms was created as boundary representation (BREP) models, which defined with non-uniform rational B-spline (NURBS) and polygon mesh surfaces (see Figure 1). The fetal masses of the phantoms were conformed to the interpolated data reported by International Commission on Radiological Protection (ICRP) Publication 89 [11]. In order to import the models to Monte Carlo n-particle transport code (MCNPX version 2.6.0), we converted them to voxelized phantoms with two different voxel sizes. The coarse voxels ($1.775 \times 1.775 \times 4.84 \text{ mm}^3$) belong to the whole maternal body except the fetal part, which is defined with the fine voxels of 16-times smaller and 128-times smaller, respectively for the models at first trimester and the two last trimesters of gestation.

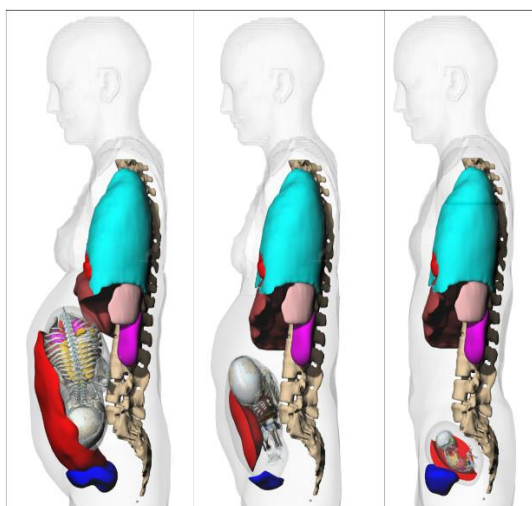


Figure 1. The series of reference pregnant phantoms based on ICRP adult female phantom [8].

Monte Carlo-based S-factors for ^{18}F

One of the two affecting factors on internal radiation dose is known as the S-factor. The S-factor is defined as the mean absorbed dose to the target organ per radionuclide disintegration in the source organ [12]. Therefore, the S factor depends not only on the geometry of the source and target organs, i.e. shape and distance, but also on the characteristics of materials in between. Computational phantoms specify these properties. Using the Monte Carlo method, the S-factors are evaluated. Therefore, the S factors also depend on the radiation transport algorithm, cross-sections and decay spectrum of the radionuclide.

MCNPX 2.6 Monte Carlo code [13] was used to calculate the S factors. In this respect, both positrons and secondary particles including photons and electrons were transported (using the so-called MODE P E card). Because the positrons are charged particles, the +F6 tallies were used to score energy deposited per unit of target mass (MeV/g) which was converted to the S factor as below:

$$S(T \leftarrow S) \left[\frac{\text{mGy}}{\text{MBq}\cdot\text{h}} \right] = \text{Tally} \left[\frac{\text{MeV}}{\text{g}} \right] \times Y_{\beta+} \times C \left[\frac{\text{mGy/MBq}\cdot\text{h}}{\text{MeV/g}} \right] \quad (1)$$

where $Y_{\beta+}$ is the positron yield of ^{18}F and $C = 1.602 \times 10^{-1} \times 3600$ is the constant value converting MeV/g to mGy/MBq·h. In our simulations, the decay data of ^{18}F was obtained from supplementary data of ICRP Publication 107 [14]. A total of 10^7 positron histories (number of particles, NPS card) were approximately simulated to reduce the statistical uncertainty below 3% in most target organs. The source regions were defined according to the Biokinetic data; the maternal brain, heart wall, kidneys, liver, lungs, bladder contents, placenta, amniotic fluid, and other tissues, in addition to the fetal body. The target region was the total fetal body and its separated organs and tissues.

Biokinetic data of ^{18}F -FDG

The Biokinetic data for maternal organs is extracted from ICRP Publication 128 [15]. Several studies previously reported the fetal uptakes of ^{18}F -FDG, and subsequently the fetal time-integrated activities based on human or animal PET scans [16-21]. The fetal ^{18}F -FDG uptake from human data was previously collected by Zanotti-Fregonara et al. [16, 7]. A sigmoidal curve was fitted to the Zanotti-Fregonara et al. data. In order to take into account, the variation of time-integrated activities, both confidence and prediction bands (95%) were extracted from the Origin software. The concentration of radioactive material in the placenta, amniotic fluid and umbilical cord were assumed to be similar to that for maternal other organs and tissues. Therefore, the time-integrated activities for these organs were calculated.

Moreover, several investigators claimed that the time-integrated activity of the fetus could be evaluated by considering (1) Similar concentrations in maternal source organs (heterogeneous), (2) Concentrations calculated based on the ratios reported by Benveniste et

al. [22] (heterogeneous), and (3) Similar concentrations in maternal other organs and tissues (homogenous). Xie and Zaidi [23-24] assumed the homogenous assumption (#3) while mentioning the heterogeneous assumptions in their papers. We also calculated the fetal time-integrated activities based on the above mentioned assumptions to be compared with the data based on human data [16, 7].

Internal dose estimates

Using the MC-based S factors and the Biokinetic data specified in the two previous subsections, we are able to estimate internal dose coefficients to various target organs and tissues (d_T) given in mGy/MBq as:

$$d_T \left[\frac{\text{mGy}}{\text{MBq}} \right] = \sum_S \frac{\tilde{A}_S}{A_0} \left[\frac{\text{Bq} \cdot \text{h}}{\text{Bq}} \right] S(T \leftarrow S) \left[\frac{\text{mGy}}{\text{MBq} \cdot \text{h}} \right] \quad (2)$$

where \tilde{A}_S/A_0 is the time-integrated activity of source organ (S) per unit administered activity comes in units of time (hours), and $S(T \leftarrow S)$ is the S factor from a source organ (S) to a target organ (T) given in mGy/MBq·h. The contributions from different source regions are also the product of $\tilde{A}_S/A_0 \times S(T \leftarrow S)$, i.e. the terms of summation demonstrated in equation 2.

Results

The fetal time-integrated activity

The time-integrated activities from Zanotti-Fregonara et al. [16] were plotted in figure 2, their data excluding the point at 28 weeks of gestation (the open circle symbol) was fitted with a sigmoidal Boltzmann curve of the form:

$$y = \frac{A_1 - A_2}{1 + e^{(x-x_0)/dx}} + A_2 \quad (3)$$

where $A_1 = 0.00321 \pm 0.00127$ (Bq h/Bq), $A_2 = 0.05346 \pm 0.00228$ (Bq h/Bq), $x_0 = 24.24026 \pm 0.34856$ (weeks) and $dx = 2.02223 \pm 0.34961$ (weeks). Also, statistical analysis of the experimental fetal time-integrated

activities is presented in this figure based on 95% confidence and prediction bands. These bands show the uncertainty in determining the mean value and where you can expect to see the next sampled data point. These bands show the extreme values that could be assumed for fetal time-integrated activity at a given gestational stage (Table 1).

Moreover, figure 2 also indicates the time-integrated activities obtained based on the three assumptions mentioned in section 2.3. It shows that the data based on assumptions #1 to #3 are not essentially correct for later stages of pregnancy, particularly in the third trimester of pregnancy, which leads to overestimating fetal time-integrated activity up to 3-times.

The ^{18}F S factors for these series of computational phantoms

The S factors for ^{18}F within 10 source organs including, maternal brain, liver, heart wall, kidneys, lungs, urinary bladder content, and other organs as well as, placenta, amniotic fluid, and the fetus were obtained in this study to be used in absorbed dose estimation. The amounts of S (fetus \leftarrow source organ) factors related to radionuclide within maternal urinary bladder content and the fetus were plotted in figure 3 in comparison with those reported by Xie and Zaidi [23]. The other studies did not report their S factors to be compared in this figure. It shows an apparent good agreement between the patterns of S factors decreasing with the gestational stage. However, the vertical axis is in logarithmic scale and the difference between two points may be much more than it seems. For example, the S (fetus \leftarrow urinary bladder content) factor from our data is about half of that from [23].

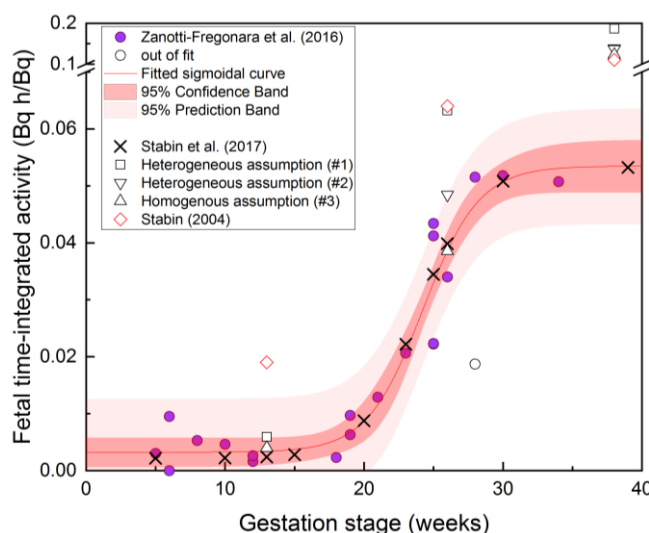


Figure 2. Sigmoidal fitted curve, 95% confidence and prediction bands for time-integrated activities reported by literature. The open symbols are excluded from fitting. The cross symbols are fitted points reported by Stabin et al. [6].

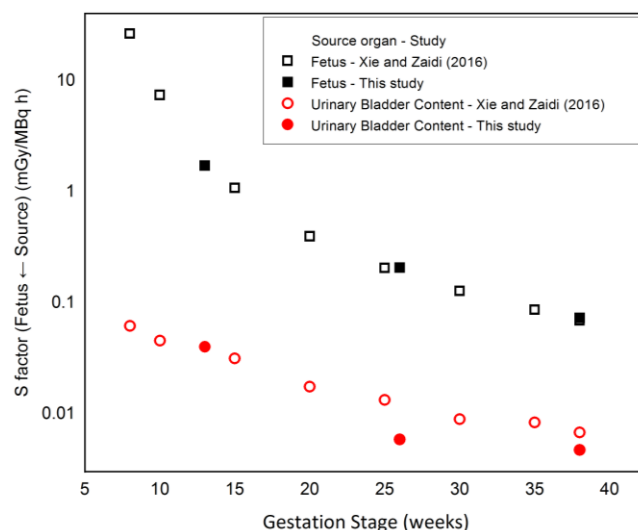


Figure 3. The self and cross S factors obtained in this study in comparison with those from Xie and Zaidi [22]. The statistical errors of our estimated S factors shown in this figure was below 0.1%.

Table 1. The fetal time-integrated activities (Bq.h/Bq) extracted from figure 2 to be used in the estimation of fetal dose variation due to biokinetic data

Stage of gestation	Fetal time-integrated activity (Bq.h/Bq)				
	From fitted curve	Confidence interval		Prediction interval	
		min	max	min	max
3 month (13 week)	3.32E-03	8.43E-04	5.80E-03	0.00E+00	1.29E-02
6 month (26 week)	3.86E-02	3.51E-02	4.21E-02	2.87E-02	4.85E-02
9 month (38 week)	5.35E-02	4.80E-02	5.90E-02	4.27E-02	6.42E-02

Table 2. The estimated fetal dose coefficients (mGy/MBq) and range of confidence/prediction intervals

Stage of gestation	Mean value	Range of 95% confidence interval		Range of 95% prediction interval	
3 month (13 week)	2.30E-02	1.87E-02	2.72E-02	1.73E-02	3.93E-02
6 month (26 week)	1.53E-02	1.45E-02	1.60E-02	1.32E-02	1.73E-02
9 month (38 week)	1.02E-02	9.77E-03	1.06E-02	9.39E-03	1.10E-02

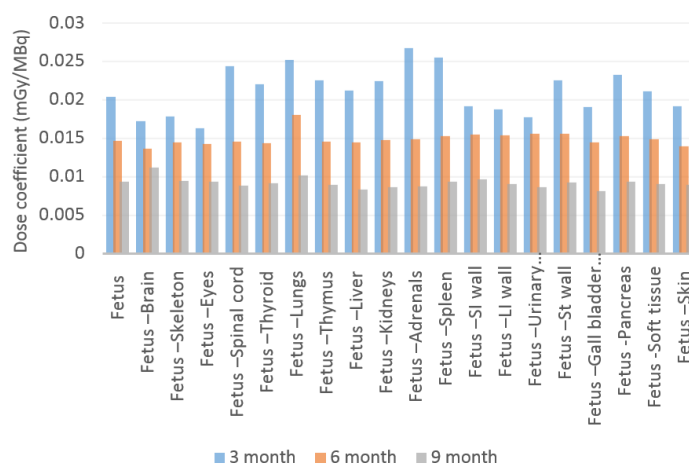


Figure 4. The dose coefficients for separated fetal organs at 3rd, 6th, and 9th month of gestation.

Absorbed doses due to intake of ^{18}F -FDG

The fetal absorbed doses due to intravenously injection of 1 MBq of ^{18}F -FDG to the mother were estimated $2.30\text{E}-2$, $1.53\text{E}-2$, and $1.02\text{E}-2$ mGy, respectively, for 3, 6, and 9 month of gestation. The mean values of dose coefficients (mGy/MBq) and their related confidence and prediction intervals were tabulated in table 2. The dose coefficients (mGy/MBq) for each separated fetal organ are also shown in figure 4. For a typical injection of 300 MBq (see table 3), the absorbed doses are 6.89, 4.85, and 3.05 mGy which all of them are below the 10 mGy threshold in which a risk (0.06% per mGy) of leukemia or childhood cancer exists following in-utero exposure [25]. However, if we consider the upper level of prediction interval, only the fetal absorbed dose in the first trimester (11.8 mGy) exceeds 10 mGy. This is equivalent to a risk of 1 cancer death per 2,000 children exposed in-utero to 11.8 mGy. Of course, the risk of occurrence of congenital anomalies is considerably higher and is about 50-100 mGy.

Contribution of source organs. Figure 5 indicates the contributions of source organs to the fetal absorbed dose. It shows that self-dose contributes to fetal dose from 25% for 3 month fetus up to 52% for the fetus at the second trimester of gestation. This figure shows that the main maternal source organs are “other organs and tissues” and “urinary bladder content”.

Comparison with literature. Figure 6 shows the fetal absorbed doses estimated in this study with its two error bars related to the uncertainties on biokinetic data (i.e. fetal time-integrated activity). In comparison with our data, all the previously reported fetal doses were plotted. This figure shows a good agreement between our reported data and those from Xie and Zaidi [23-24] at first and second trimesters, while that for third trimester is ~30% smaller compared to Xie and Zaidi [23-24]. Almost all the other estimated fetal doses are well below the error bars considered for biokinetic uncertainty.

Table 3. The estimated fetal dose (mGy) assuming a typical of 300 MBq administered activity

Stage of gestation	Mean value	Range of 95% confidence interval		Range of 95% prediction interval	
3 month (13 week)	6.89	5.62	8.16	5.18	11.80*
6 month (26 week)	4.58	4.36	4.79	3.97	5.19
9 month (38 week)	3.05	2.93	3.17	2.82	3.29

* exceeds 10 mGy; the threshold for childhood cancer [24]

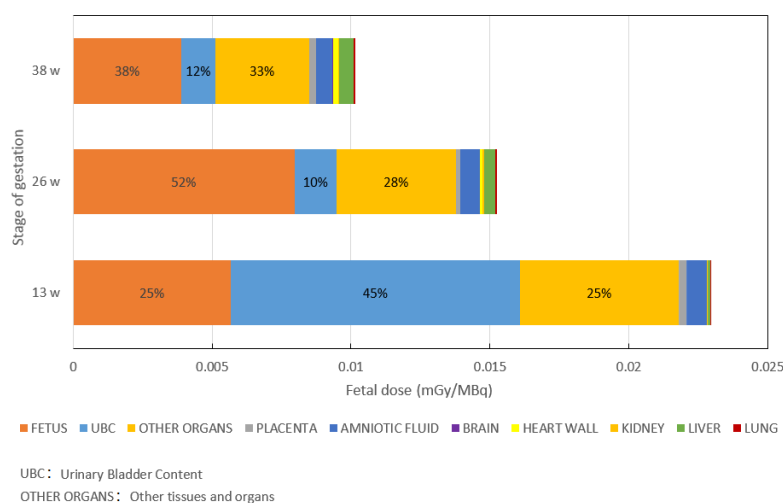


Figure 5. The contributions of source organs to fetal dose at 3rd, 6th, and 9th month of gestation

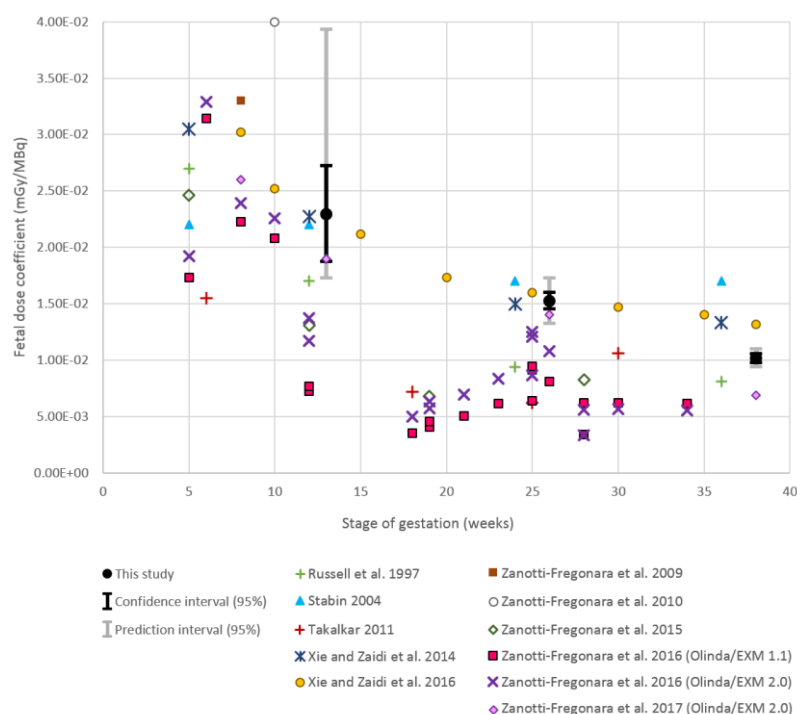


Figure 6. The fetal dose coefficients (mGy/MBq) from this study with its confidence and prediction intervals in comparison with those from literature

Discussion

As shown in figure 2, the heterogeneous assumption (#1) results in overestimated values of time-integrated activity at the two last trimesters of pregnancy, which also confirmed by Zankar-Fregonara et al. data [7]. They declared that the uptake in the fetal brain is significantly lower than the uptake in the mother's brain. Therefore, this is not essentially correct to assume the same concentration of time-integrated activity for fetal and maternal organs.

The derived time-integrated activity from heterogeneous assumption (#2) is within the prediction band at the second trimester, while at the third trimester is overestimated (~2-times). It means that data extrapolated from monkey model by Benveniste et al. [22] may not be appropriate to be applied for humans in all stages of gestation (particularly at third trimester).

The homogenous assumption (#3) which is also employed by Xie and Zaidi [23-24], obviously leads to overestimation of fetal time-integrated activities at third trimester of pregnancy. This issue may be the reason that 30% higher fetal dose at third trimester was reported by Xie and Zaidi [23-24].

By considering the prediction and confidence bands, we indicated the variation that should be taken for biokinetic data, conservatively. Nevertheless, many of data points still fall outside the given intervals (see figure 6). Therefore, a large part of the variability of fetal doses is likely due to differences between computational phantoms, either maternal or fetal parts considering their corresponding contributions to fetal doses (see figure 5). This claim is true because other studies report different contributions of source organs. For example, Xie and Zaidi found that the maternal

body contributes 36% to fetal dose, while the self-dose contributed 47 % at 30th week of gestation. These contribution percentages are similar to our data for third trimester (see figure 5). In contrast, Zankar-Fregonara et al. [21] reported that self-dose is the main contribution of fetal dose in the first trimester, while it contributes 25% in second trimester. These estimated contributions are obviously inconsistent with our findings.

In summary, by considering the variation due to Biokinetic data, we suggest that accurate fetal dosimetry is relevant only in the early and first trimester of pregnancy. Beyond this period, variations of fetal doses related to the radiopharmaceutical biokinetic is well below safe intervals (10 mGy).

More accurate fetal dosimetry could be performed using patient-specific data of fetal time-integrated activity from PET scans and also patient-specific phantoms. Until then, the estimated variation of absorbed dose-related to biokinetic data could be helpful in the radiation protection context. The variations related to the fetal body habitus, maternal body habitus and chord length distribution between the fetus and maternal urinary bladder content will be taken into account in our future investigations.

Conclusion

In this study we evaluated the reasonable range of fetal time-integrated activities for ¹⁸F-FDG injected to the mother. By doing this, we could estimate the variation of fetal doses due to the biokinetic of the mother. However, the variation of fetal dose due to fetal and maternal body habitus and fetal positioning inside the gravid uterus are remained for further investigation in our next studies.

References

1. Mankoff DA, Dehdashti F, Shields AF. Characterizing tumors using metabolic imaging: PET imaging of cellular proliferation and steroid receptors. *Neoplasia*. 2000 Jan 1;2(1-2):71-88.
2. Bruzzi JF, Munden RF, Truong MT, Marom EM, Sabloff BS, Gladish GW, Iyer RB, Pan TS, Macapinlac HA, Erasmus JJ. PET/CT of esophageal cancer: its role in clinical management. *Radiographics*. 2007 Nov;27(6):1635-52.
3. Chung HH, Jo H, Kang WJ, Kim JW, Park NH, Song YS, Chung JK, Kang SB, Lee HP. Clinical impact of integrated PET/CT on the management of suspected cervical cancer recurrence. *Gynecologic oncology*. 2007 Mar 1;104(3):529-34.
4. Groheux D, Espié M, Giacchetti S, Hindié E. Performance of FDG PET/CT in the clinical management of breast cancer. *Radiology*. 2013 Feb;266(2):388-405.
5. Leide-Svegborn S. Radiation exposure of patients and personnel from a PET/CT procedure with 18F-FDG. *Radiation protection dosimetry*. 2010 Apr 1;139(1-3):208-13.
6. Ishiguro T, Nishikawa N, Ishii S, Yoshihara K, Haino K, Yamaguchi M, Adachi S, Watanabe T, Soeda S, Enomoto T. PET/MR imaging for the evaluation of cervical cancer during pregnancy. *BMC Pregnancy and Childbirth*. 2021 Dec;21(1):1-7.
7. Zanutti-Fregonara P, Stabin MG. New Fetal Radiation Doses for 18F-FDG Based on Human Data. *Journal of Nuclear Medicine*. 2017 Nov 1;58(11):1865-6.
8. Rafat-Motavalli L, Miri-Hakimabad H, and Hoseinian-Azghadi E. Fetal and maternal dose assessment for diagnostic scans during pregnancy. *Phys Med Biol*. 2016;61(9):3596-3608.
9. Rafat-Motavalli L, Miri-Hakimabad H, Hoseinian-Azghadi E. Hybrid pregnant reference phantom series based on adult female ICRP reference phantom. *Radiation Physics and Chemistry*. 2018 Mar 1;144:386-95.
10. Hoseinian Azghadi E, Rafat Motavalli L, and Miri Hakimabad H. Development of a 9-month pregnant hybrid phantom and its internal dosimetry for thyroid agents. *J Radiat Res*. 2014a;55(4):730-747.
11. ICRP, 2002. Basic Anatomical and Physiological Data for Use in Radiological Protection Reference Values. ICRP Publication 89. Ann. ICRP 32 (3-4).
12. Bolch WE, Eckerman KF, Sgouros G, Thomas SR. MIRD pamphlet no. 21: a generalized schema for radiopharmaceutical dosimetry—standardization of nomenclature. *Journal of Nuclear Medicine*. 2009 Mar 1;50(3):477-84.
13. Hendricks JS, McKinney GW, Fensin ML, James MR, Johns RC, Durkee JW, Finch JP, Pelowitz DB, Waters LS, Johnson MW, Gallmeier FX. MCNPX 2.6.0 Extensions. Los Alamos National Laboratory. 2008 Apr 11.
14. ICRP, 2008. Nuclear Decay Data for Dosimetric Calculations. ICRP Publication 107. Ann. ICRP 38 (3).
15. ICRP, 2015. Radiation Dose to Patients from Radiopharmaceuticals: A Compendium of Current Information Related to Frequently Used Substances. ICRP Publication 128. Ann. ICRP 44(2S).
16. Zanutti-Fregonara P, Chastan M, Edet-Sanson A, Ekmekcioglu O, Erdogan EB, Hapdey S, Hindie E, Stabin MG. New fetal dose estimates from 18F-FDG administered during pregnancy: standardization of dose calculations and estimations with voxel-based anthropomorphic phantoms. *Journal of Nuclear Medicine*. 2016 Nov 1;57(11):1760-3.
17. Stabin MG. Proposed addendum to previously published fetal dose estimate tables for 18F-FDG. *Journal of Nuclear Medicine*. 2004 Apr 1;45(4):634-5.
18. Zanutti-Fregonara P, Champion C, Trébossen R, Maroy R, Devaux JY, Hindié E. Estimation of the β + dose to the embryo resulting from 18F-FDG administration during early pregnancy. *Journal of Nuclear Medicine*. 2008 Apr 1;49(4):679-82.
19. Zanutti-Fregonara P, Jan S, Champion C, Trébossen R, Maroy R, Devaux JY, Hindié E. In vivo quantification of 18F-FDG uptake in human placenta during early pregnancy. *Health physics*. 2009 Jul 1;97(1):82-5.
20. Zanutti-Fregonara P, Jan S, Taieb D, Cammilleri S, Trébossen R, Hindié E, Mundler O. Absorbed 18F-FDG dose to the fetus during early pregnancy. *Journal of Nuclear Medicine*. 2010 May 1;51(5):803-5.
21. Zanutti-Fregonara P, Koroscil TM, Mantil J, Satter M. Radiation dose to the fetus from [18F]-FDG administration during the second trimester of pregnancy. *Health physics*. 2012 Feb;102(2):217.
22. Benveniste H, Fowler JS, Rooney WD, Moller DH, Backus WW, Warner DA, Carter P, King P, Scharf B, Alexoff DA, Ma Y. Maternal-fetal in vivo imaging: a combined PET and MRI study. *Journal of Nuclear Medicine*. 2003 Sep 1;44(9):1522-30.
23. Xie T, Zaidi H. Development of computational pregnant female and fetus models and assessment of radiation dose from positron-emitting tracers. *European journal of nuclear medicine and molecular imaging*. 2016 Dec 1;43(13):2290-300.
24. Xie T, Zaidi H. Fetal and maternal absorbed dose estimates for positron-emitting molecular imaging probes. *Journal of Nuclear Medicine*. 2014 Sep 1;55(9):1459-66.
25. Doll R, Wakeford R. Risk of childhood cancer from fetal irradiation. *The British journal of radiology*. 1997 Feb;70(830):130-9.